Hindawi Publishing Corporation
Mathematical Problems in Engineering
Volume 2012, Article ID 769385, 22 pages
doi:10.1155/2012/769385

Research Article

Stochastic Inverse Identification of Nonlinear Roll Damping Moment of a Ship Moving at Nonzero-Forward Speeds

S. L. Han and Takeshi Kinoshita

Institute of Industrial Science, The University of Tokyo, 4-6-1 Komaba, Meguro-ku, Tokyo 153-8505, Japan

Correspondence should be addressed to Takeshi Kinoshita, kinoshita@iis.u-tokyo.ac.jp

Received 1 August 2012; Revised 14 November 2012; Accepted 26 November 2012

Academic Editor: Fatih Yaman

The nonlinear responses of ship rolling motion characterized by a roll damping moment are of great interest to naval architects and ocean engineers. Modeling and identification of the nonlinear damping moment are essential to incorporate the inherent nonlinearity in design, analysis, and control of a ship. A stochastic nonparametric approach for identification of nonlinear damping in the general mechanical system has been presented in the literature (Han and Kinoshits 2012). The method has been also applied to identification of the nonlinear damping moment of a ship at zero-forward speed (Han and Kinoshits 2013). In the presence of forward speed, however, the characteristic of roll damping moment of a ship is significantly changed due to the lift effect. In this paper, the stochastic inverse method is applied to identification of the nonlinear damping moment of a ship moving at nonzero-forward speed. The workability and validity of the method are verified with laboratory tests under controlled conditions. In experimental trials, two different types of ship rolling motion are considered: time-dependent transient motion and frequency-dependent periodic motion. It is shown that this method enables the inherent nonlinearity in damping moment to be estimated, including its reliability analysis.

1. Introduction

Ship motions are defined by the six degrees of freedom that a ship can experience at sea. Among them, rolling motion, which is defined by a rotational motion around the longitudinal axis of a ship, has been attracting considerable research attention over the years because large roll motions might be a serious threat to the safety of a ship such as ship capsizing or structure failure. Therefore, an appropriate model to describe the rolling motion is crucial for accurate predictions of ship's roll response in a given sea state.

There are considerable studies on the modeling of the rolling motion [1–20]. The rolling motion of a ship can be characterized by analyzing components of moments such as moment of inertia, damping and restoring moments. Among them, the roll damping moment is considered as the most important component due to difficulties in identifying its value. The difficulties result from its nonlinearity due to the fluid viscosity and its dependence on the forward speed. The usual practice of identifying roll damping moment of a ship is to use the parametric method [8–14], which assumes the form of nonlinearity a priori. The coefficients of the prescribed form of nonlinearity are then estimated by relating the loss in potential energy over each cycle of the roll decay test with the energy dissipation as the damping. This method gives quite accurate result but sometimes fails when one adopt inaccurate nonlinear model because different types of nonlinear model produce different motion responses [15].

A large number of studies on this subject have been concentrated on the parametric identification mentioned above. In contrast, there are few studies involving nonparametric identification where the prior knowledge for the nonlinearities of damping moments is not necessary. For example, Haddara and Hinchey [16] proposed a method, based on the combination of the neural networks technique with the standard parametric identification, for modeling nonlinear damping moment from free-roll decay curve. They also applied the method to random roll responses measured during the sea trials to investigate roll characteristics of full-scale ships at sea [17]. Roberts and Vasta [18] presented a stochastic method for estimating the damping moment and the excitation spectrum using the Markov model for the energy envelope of the response.

In recent years, inverse methods have been presented [1, 2, 19, 20] for the nonparametric identification of damping moment of a ship. Conceptually, these methods are based on inverse formalism originated from the transformation of an original nonlinear motion equation for ship rolling motion in either a deterministic [19, 20] or stochastic manner [1, 2]. The roll damping moment of a ship at zero-forward speed was identified from the measurement of the responses of the system based on the inverse problem formulation [2, 20], which is ill-posed in the sense that small variations in the input data can result in erroneous inverse solution. Compared with the deterministic inverse method [19, 20], the stochastic inverse method [1, 2] is robust and reliable in the sense that it can also provide a reliability analysis of the identified results.

In the literature [2], the study on the application of the stochastic inverse method was presented for the case of zero-forward speed. The inherent nonlinearity in damping moment of a test ship at zero-forward speed was successfully identified, including its credible intervals as an indicator of reliability of identification. However, there is no guarantee that the method can be applied to the case of nonzero-forward speed since the nonlinear characteristic of roll damping has changed significantly due to the lift effect in the presence of the forward speed. It is well known that the roll damping moment of a ship is also strongly dependent on the forward speed [14].

In this paper, attention is focused on the real practical application of the stochastic inverse method [1] to identification of nonlinear damping moment of a ship moving with "non-zero" forward speeds. For this purpose, we first derive a stochastic inverse model by defining nonlinear damping moment as a nondeterministic parameter, which is multivariate random variable. This stochastic inverse modeling method is then applied to the laboratory tests to assess workability and practicability. Two different motions, transient motion and forced periodic motion, are considered with various trial conditions. The unique features of the method can be summarized in the following sense: firstly, it is nonparametric, that is, it does not require a prescribed form of nonlinearity unlike the conventional parametric

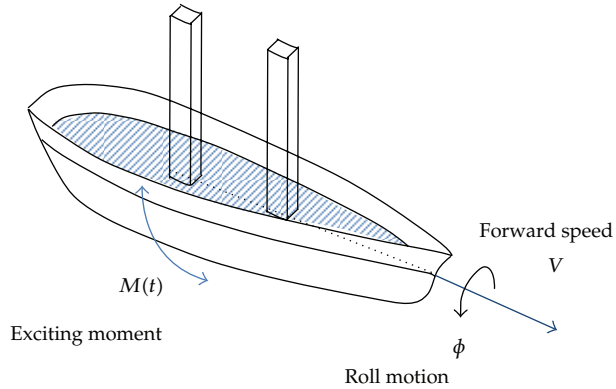

Figure 1: The schematic of the experiment.

methods. Secondly, it also offers a way of quantification of confidence level of identified solution given noisy data since the method is based on a stochastic inverse model.

The outline of this paper is as follows. The stochastic inverse model for nonlinear damping of a ship is derived in Section 2. Experimental setups are explained in Section 3. Section 4 presents analysis results of experimental data. Concluding remarks are made in Section 5.

2. Problem Formulation

2.1. Governing Equation for Ship Rolling Motion

It is assumed that the rolling motion ϕ of a ship moving at a forward speed V, illustrated in Figure 1, is governed by the following nonlinear differential equation of motion:

$$(I + \Delta I)\ddot{\phi}(t) + B\left(\phi, \dot{\phi}; t\right) + K\left(\phi; t\right) = M(t), \tag{2.1}$$

where I is the actual mass moment of inertia, ΔI is the added mass moment of inertia, $B(\phi, \dot{\phi})$ is the nonlinear roll damping moment, $K(\phi)$ is the restoring moment, and $M(t)$ is the roll-excitation moment. In the above equation, an overdot denotes a differentiation with respect to time.

The roll damping moment is expressed as a positive nonlinear function of the roll angle and angular velocity. The roll damping moment $B(\phi, \dot{\phi})$ is also affected by the forward speed of the ship since a lift effect occurs due to the presence of the forward speed. The restoring moment $K(\phi)$, which is expressed as an antisymmetric function of the roll angle, is induced by hydrostatic pressure exerted by a fluid at equilibrium due to the force of gravity. If the amplitude of roll angle is sufficiently small, then it is often expressed as the multiplication of the displacement of a ship and the distance between metacentric height and center of gravity GM, that is, $K(\phi) = \rho g \nabla \cdot \mathrm{GM}\phi$. In this study, our attention is restricted to the small amplitude motion.

2.2. Inverse Setting for the Nonlinear Damping Moment

From the mathematical manipulation based on the concept of variation of parameters, the following relationship is obtained [1, 2, 19, 20]:

$$g(\phi;t) = \int_0^t \frac{x_1(\tau)x_2(t) - x_1(t)x_2(\tau)}{(I+\Delta I)W(\tau)}\{B(\phi,\dot{\phi};t)\}d\tau, \tag{2.2}$$

where $W \equiv |x_1\dot{x}_2 - x_2\dot{x}_1|$ and x_1, x_2 are chosen to satisfy the following equations, respectively:

$$\begin{aligned}(I+\Delta I)\ddot{x}_1 + \rho g\nabla\cdot \mathrm{GM}x_1 = 0, \quad x_1(0)=1,\ \dot{x}_1(0)=0,\\ (I+\Delta I)\ddot{x}_2 + \rho g\nabla\cdot \mathrm{GM}x_2 = 0, \quad x_2(0)=0,\ \dot{x}_2(0)=1.\end{aligned} \tag{2.3}$$

The left hand side of (2.2) is given by

$$g(\phi;t) = \phi(t) - \alpha x_1(t) - \beta x_2(t) - \int_0^t \frac{x_1(\tau)x_2(t) - x_1(t)x_2(\tau)}{(I+\Delta I)W(\tau)}M(\tau)d\tau, \tag{2.4}$$

where $\alpha = \phi(0)$ and $\beta = \dot{\phi}(0)$.

The purpose of the study is to inversely identify the nonlinear damping moment given a measured response data ϕ. For a set of measured roll response data $\phi_i = \phi(t_i)$ during $0 < t < T$, the following system is given for the unknown nonlinear damping $B_j = B(\tau_j)$, $j = 1, \ldots, n$:

$$g_i = \sum_{\tau_j < t_i} H_{ij}B_j, \quad i = 1, \ldots, m, \tag{2.5}$$

where

$$H_{ij} = \Delta\tau\frac{x_1(\tau_j)x_2(t_i) - x_1(t_i)x_2(\tau_j)}{(I+\Delta I)W(\tau_j)}, \tag{2.6}$$

$$g_i = \phi(t_i) - \alpha x_1(t_i) - \beta x_2(t_i) - \sum_{\tau_j < t_i}\Delta\tau\frac{x_1(\tau_j)x_2(t_i) - x_1(t_i)x_2(\tau_j)}{(I+\Delta I)W(\tau_j)}M(\tau_j). \tag{2.7}$$

The identification of the nonlinear damping can be achieved by inverting the matrix system (2.5) from the observable parameter g_i. This identification procedure can be considered as the inverse problem [21–23] since its aim is to find the cause from the effect of the physically observable data.

It is worth noting that the system (2.5) is given by discretizing the first-kind integral operator (2.2). According to the inverse problem theory [21–23], the inverse of such systems is very sensitive to small changes in the data. The data-driven nature of the inverse problem makes the inverse analysis more difficult because one should use the measured data containing random errors arising from various sources of noise in the inverse setting. For such systems, which are often called ill-posed, the usual inverse procedure yields erroneous solutions which are physically meaningless.

2.3. Stochastic Inversion

To ensure a stable solution procedure, the unknown damping moment $B(\phi, \dot{\phi}; t)$ will here be modeled as a sequence of random variable $U(t; \xi)$, $U : \Omega \to \mathbb{R}^n$, where ξ is every possible outcome of an arbitrary nonempty sample space Ω. Then, the random variable U can be related to the directly observable quantity g by the Bayesian formula [23]:

$$p(U \mid g) \propto p(g \mid U)p(U), \tag{2.8}$$

where $p(g \mid U)$ is the likelihood, $p(U)$ is the prior probability density function, and $p(U \mid g)$ is the posterior probability density function.

Using adequate probabilistic models, the probabilistic expression (2.8) can be specified more clearly. In the case where the measurement error is independent additive Gaussian random noise with zero mean and standard deviation σ, the likelihood $p(g \mid U)$ has the form:

$$p(g \mid U) \propto \left(\sigma^2\right)^{-m/2} \exp\left(-\frac{\|HU - g\|_2^2}{2\,\sigma^2}\right), \tag{2.9}$$

where $\|\cdot\|_2$ refers to Euclidean norm, and m is the number of measurements. Using a pairwise Markov random field model [23–25], the prior $p(U)$ can be written as

$$p(U) \propto \lambda^{n/2} \exp\left(-\frac{\lambda}{2} U^T W U\right), \tag{2.10}$$

where the matrix $W \in \mathbb{R}^{n \times n}$ is defined by

$$W_{ij} = \begin{cases} n_i, & i = j, \\ -1, & i \sim j, \\ 0, & \text{otherwise}, \end{cases} \tag{2.11}$$

where n_i is the number of neighbors for the point i, and $i \sim j$ means that i and j are adjacent. Thus, (2.8) can be specified as

$$p(Ug) \propto \left(\sigma^2\right)^{-m/2} \exp\left(-\frac{\|HU - g\|_2^2}{2\sigma^2}\right) \lambda^{n/2} \exp\left(-\frac{\lambda}{2} U^T W U\right). \tag{2.12}$$

The parameters σ and λ for the probabilistic model are also nondeterministic and difficult to be known a priori. In the stochastic inversion, these uncertainties are naturally resolved by expanding into the hierarchical model [23–25]:

$$p(U, \lambda, \sigma \mid g) \propto \left(\sigma^2\right)^{-(m/2+\alpha_2+1)} \exp\left(-\frac{\|HU - g\|^2 + 2\beta_2}{2\sigma^2}\right) \lambda^{(n/2+\alpha_1-1)} \exp\left(-\frac{\lambda(U^T W U + \beta_1)}{2}\right), \tag{2.13}$$

where $(\alpha_1,\ \beta_1)$ is a pair of gamma distribution for λ, and $(\alpha_2,\ \beta_2)$ is a pair of inverse gamma distribution for the prior of σ. Based on the hierarchical model (2.13), it is possible to determine, at the same time, the stable inverse solution and the hyperparameters σ and λ through a numerical sampling technique such as Markov chain Monte Carlo [1, 23–25].

2.4. MCMC Simulation

To extract information on the damping moment from the constructed stochastic inverse model, it is necessary to employ the simulation technique such as Markov chain Monte Carlo, whose aim is to draw an identical independent distributed set of samples from a target density. The hierarchical model (2.13) with the given observable quantities can be explored by the following hybrid algorithm which is designed by mixing Metropolis-Hastings steps in the Gibbs sampler [1, 23–26].

(i) Initialize $U^{(0)} = \{U_1^{(0)}, U_2^{(0)}, \ldots, U_n^{(0)}\}$, $\lambda^{(0)}$, and $\sigma^{(0)}$.

(ii) For $i = 0 : N_{\mathrm{MCMC}} - 1$

Sample $U_1^{(i+1)}$ from $p(U_1 \mid U_2^{(i)},\ U_3^{(i)}, \ldots, U_n^{(i)}, \lambda^{(i)},\ \sigma^{(i)})$
Sample $U_2^{(i+1)}$ from $p(U_2 \mid U_1^{(i+1)},\ U_3^{(i)}, \ldots, U_n^{(i)}, \lambda^{(i)}, \sigma^{(i)})$
$\vdots$
Sample $U_n^{(i+1)}$ from $p(U_n \mid U_1^{(i+1)},\ U_2^{(i+1)}, \ldots,\ U_{n-1}^{(i+1)}, \lambda^{(i)}, \sigma^{(i)})$
Sample u_1 from the uniform distribution on $[0, 1]$
Sample $\lambda^{(*)}$ from $q(\lambda^{(*)} \mid \lambda^{(i)})$
if $u_1 < \min\{1,\ p(\lambda^{(*)} \mid U^{(i+1)},\ \sigma^{(i)}) q(\lambda^{(i)} | \lambda^{(*)}) / p(\lambda^{(i)} \mid U^{(i+1)},\ \sigma^{(i)}) q(\lambda^{(*)} \mid C\lambda^{(i)})\}$, $\lambda^{(i+1)} = \lambda^{(*)}$
else $\lambda^{(i+1)} = \lambda^{(i)}$
Sample u_2 from the uniform distribution on $[0, 1]$
Sample $\sigma^{(*)}$ from $q(\sigma^{(*)} \mid \sigma^{(i)})$
if $u_2 < \min\{1, p(\sigma^{(*)} \mid U^{(i+1)},\ \lambda^{(i+1)}) q(\sigma^{(i)} \mid \sigma^{(*)}) / p(\sigma^{(i)} \mid U^{(i+1)},\ \lambda^{(i+1)}) q(\sigma^{(*)} \mid \sigma^{(i)})\}$, $\sigma^{(i+1)} = \sigma^{(*)}$
else $\sigma^{(i+1)} = \sigma^{(i)}$.

The sampled set of realizations $\{U^{(i)}\}$ can then be used to approximate the statistics of the target densities $p(U, \lambda, \sigma \mid g)$ by

$$p(U, \lambda, \sigma \mid g) \approx \frac{1}{N_{\mathrm{MCMC}}} \sum_{k=1}^{N_{\mathrm{MCMC}}} \delta\left(U - U^{(k)}\right), \tag{2.14}$$

where N_{MCMC} is the number of Monte Carlo simulation and δ is Dirac delta function.

In summary, the damping moment of a ship moving with nonzero-forward speed can be identified through the following steps. (1) Derive the inverse model (2.5) relating the desired damping moment with the observable parameter, which is a function of the roll response; (2) measure the dynamic roll response of a ship moving at a nonzero- forward speed; (3) formulate stochastic inverse model (2.8) given the measured roll response; (4) use the designed MCMC algorithm to identify the damping moment.

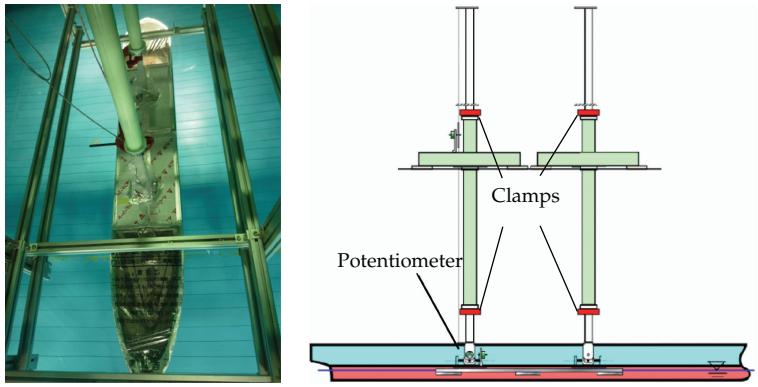

(a) (b)

Figure 2: Overview of (a) the test model and (b) experimental setups.

Table 1: Particulars of the test model.

Length L_{pp}	2.500 m
Breadth B	0.387 m
Draft D	0.132 m
Displacement volume ∇	0.110 m^3
The distance between metacentric height and center of gravity GM	0.074 m
Vertical position of the center of buoyancy KB	0.071 m
Vertical position of the transverse metacenter above the keel line KM	0.179 m
Natural frequency ω_n	6.905 rad/s (without BK) 6.136 rad/s (with BK)

3. Experimental Setup

The workability and accuracy of the present method were verified by damping moment identification of the test model. The related experiments were conducted at the Ocean Engineering (OE) Basin of the University of Tokyo. The basin, which is often called as the towing tank, is a physical water tank to perform hydrodynamic tests with ship models. Figure 2 shows the test model used for the experimental analysis and an overview of experimental setups. The plan of the test model is shown in Figure 3. Table 1 summarizes particulars of the test model. During experiments, the test model was rigidly clamped in all degrees of freedom, excepting roll motion to minimize effects from the other modes of motions.

Figure 4 shows the layout of the OE Basin, whose length, breadth, and depth are 50 m, 10 m, and 5 m, respectively. The basin is equipped with a towing carriage that runs on two rails on either side of the basin at a speed from zero to 2 m/s. The carriage is also equipped with computers and devices to measure or control the speed of the towing carriage. The test model was initially positioned in one side of the basin and then towed by the carriage to the opposite side ranging from zero to 2 m/s. The roll motions are recorded by the potentiometer attached to the center of gravity of the test model.

The model was first tested without any appendages such as bilge-keels to consider the hull damping characteristics. After that, for the purpose of assessing the workability, two

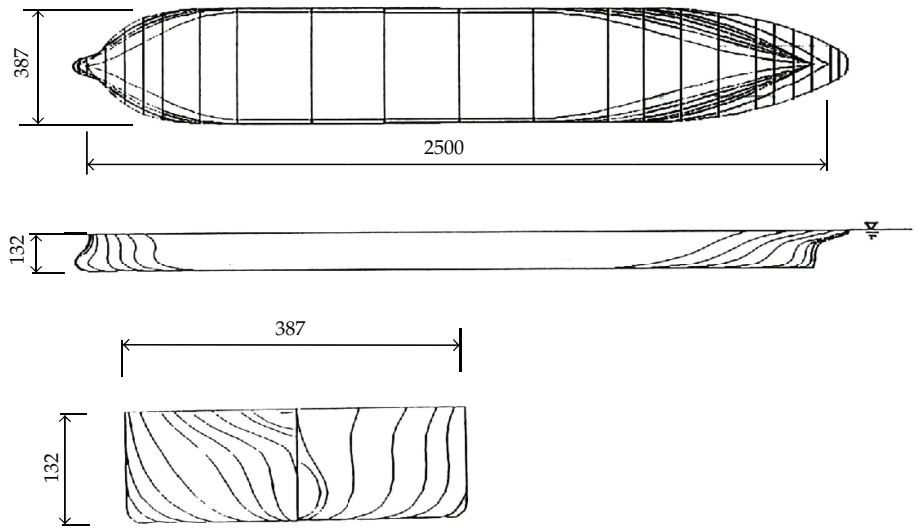

Figure 3: Body plan of the test model.

Figure 4: Layout of ocean engineering basin at the University of Tokyo.

bilge-keels (BK) with about 1 m long are attached to both sides of the test model at the turn of the bilge as in Figure 5. The installation of BK generates totally different roll characteristic since BK increases hydrodynamic resistance to rolling motion and makes the ship roll less. The effect of BK can easily observed even at zero-forward speed and becomes larger with the presence of the nonzero-forward speed.

For the experimental application, two different types of motions, time-dependent transient motion and frequency-dependent periodic motion, are considered. Firstly, the transient motion caused by an initial roll angle is considered. An external moment is first applied to the test model by static means to give an initial roll angle. Then the moment is eliminated and the decaying roll motion is measured. Secondly, the forced motion caused by a periodic excitation is considered. Monofrequency sinusoidal roll motion is first imposed by the vertical force generated by the force oscillating device in Figure 6. The resulting vertical force is recorded by the load cell and converted to the exciting moment by multiplying the moment arm.

It should be noted that a linear approximation for the restoring moment is valid only for sufficiently small roll angle. As pointed out earlier, in this study, we restrict our attention to the small amplitude motion so that the restoring moment can be expressed by the linear form.

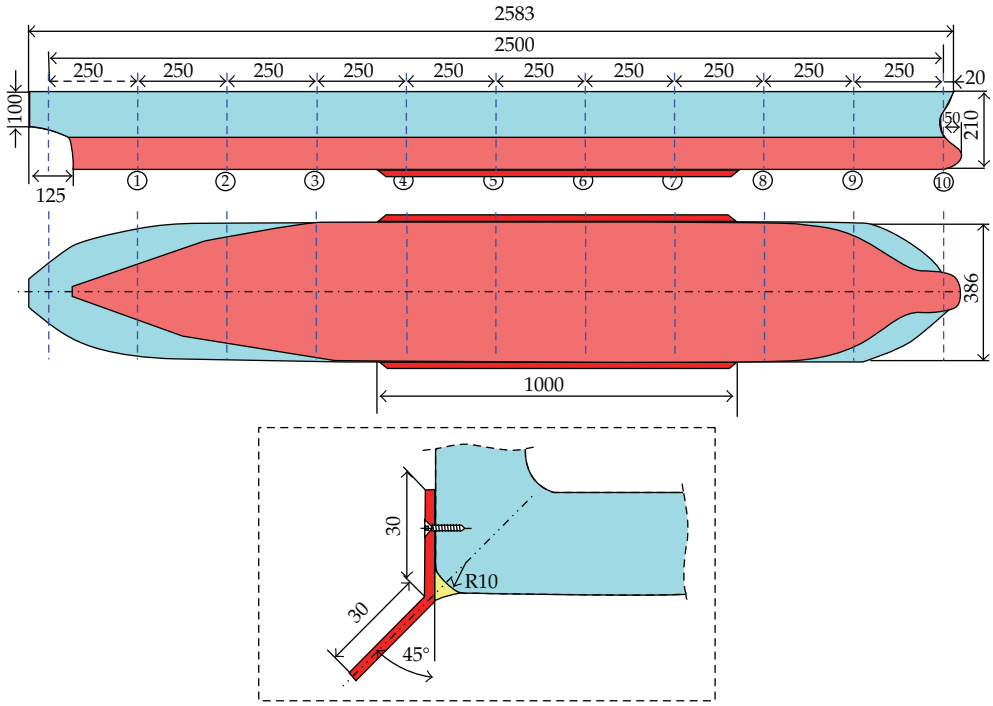

Figure 5: Attachment of bilge-keels to the both sides of the test model.

4. Analysis of Experimental Data

4.1. Transient Motion: Free-Decay Rolling

As a first application, a transient motion induced by an initial roll angle is considered. This motion is referred to as the free-decay rolling motion. For the trial, an initial roll angle is first given as $\phi(0) = \alpha$ while the test model is being towed by the carriage with a forward speed V. The static moment is then eliminated and the resultant response is recorded by measuring devices. This free-decay rolling motion is governed by the following initial value problem from (2.1) since $M(t) = 0$:

$$(I + \Delta I)\ddot{\phi} + B(\phi, \dot{\phi}) + K\phi = 0, \quad \phi(0) = \alpha,\ \dot{\phi}(0) = 0. \tag{4.1}$$

Dividing both sides of (4.1) by $I + \Delta I$, we can obtain

$$\ddot{\phi} + \tilde{B}(\phi, \dot{\phi}) + {\omega_n}^2\phi = 0, \tag{4.2}$$

where $\tilde{B} = B/(I + \Delta I)$ and $\omega_n = \sqrt{K/(I + \Delta I)}$.

Recorded roll responses are presented in Figure 7 for the test model without and with BK. Here, the Froude number (Fr) is defined by $V/\sqrt{L_{\mathrm{pp}}g}$, where V is the velocity of the test model, g is the gravitational acceleration, and L_{pp} is the length of the ship. It can be observed that responses of the test model with BK decay to zero faster than the test model without BK.

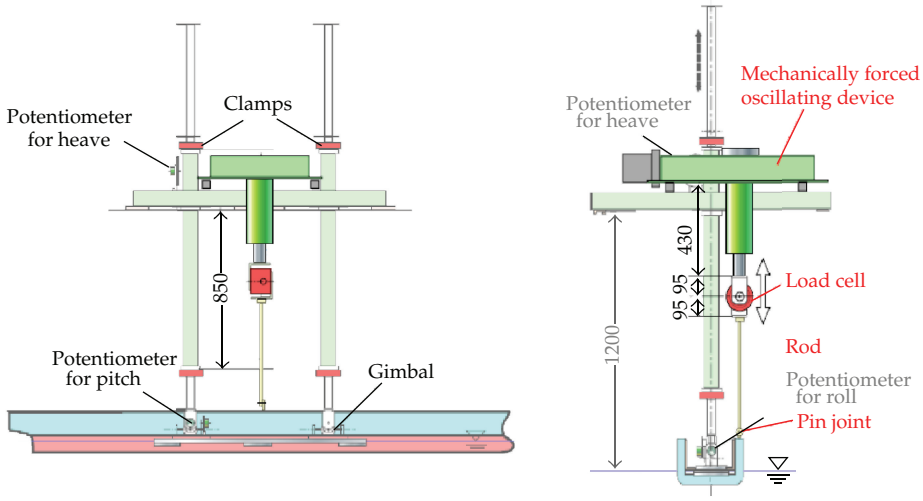

Figure 6: Forced oscillating devices: (a) side view. (b) front view.

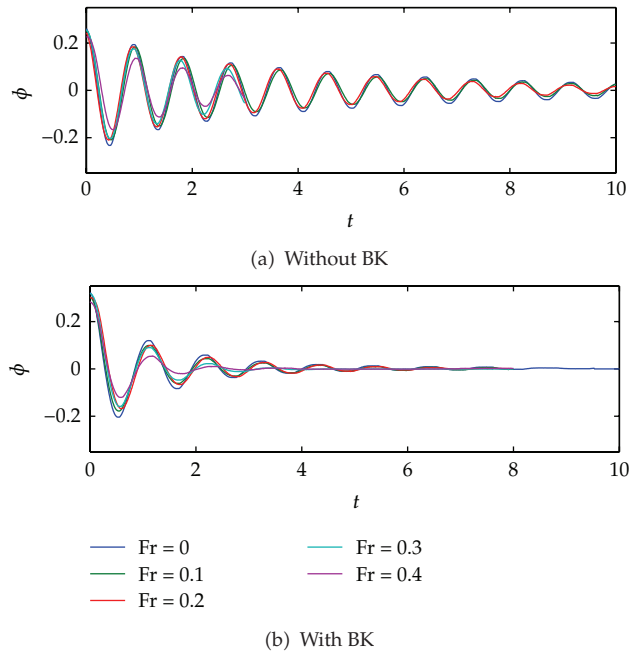

Figure 7: Roll decay curve of the test model for different forward speeds.

Moreover, the rate of decrease of roll angle becomes larger when the forward speed increases for both cases of the model without and with BK. This clearly shows that the damping is dependent on the forward speed. This fact is well known and described in various papers [14, 27].

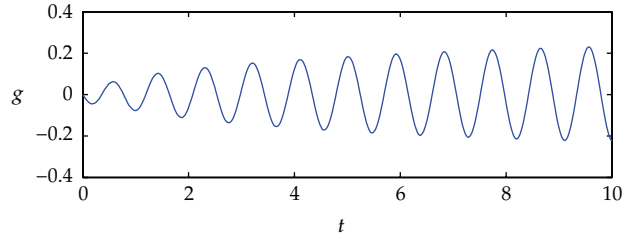

(a) Without BK

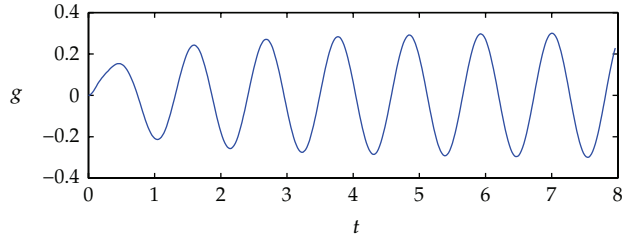

(b) With BK

Figure 8: The converted quantity g from the measured roll-angle data when Fr = 0.2.

It is worthwhile to note that the physical coefficients are not necessary for the case of free-decay rolling. The only thing that is required for applying the present method is the natural angular frequency. The natural frequency for the test model is shown in Table 1. The variation of the roll natural frequency due to the addition of bilge keels is extremely large. In this study, for simplicity, the frequency of the largest Fourier component is considered as the natural frequency for the BK model.

To illustrate the method, through application to experimental data in Figure 7, a particular case of the roll-angle data with Fr = 0.2 was chosen. As a first stage of the identification, the roll-angle data set ϕ_i $(i = 1, 2, \ldots, m)$ is converted to a set of the observable quantity g_i using the relationship given by (2.7). This is clearly straightforward if the roll angle is recorded since the excitation moment $M(t)$ is zero for the case of the free-decay rolling motions. Consequently, the observable quantity can be computed by $g_i = \phi_i - \alpha x_1(t_i)$ and the results are shown in Figure 8. Using this quantity, we can construct a stochastic inverse model $p(U, \lambda, \sigma \mid g)$ for both cases of experiments.

Before illustrating results from MCMC simulation, the least-squares estimation for the inverse solution of (2.5) is first presented in Figure 9. The results clearly show the difficulties with the standard inverse solution to (2.5), that is, lack of stability in solution. The instability, frequent sign changes, is often encountered in solving data-driven inverse problems since the inevitable errors, no matter how small, incurred in taking and analyzing measured signal, are the main reason of this instability.

We consider now the stochastic inverse model $p(U, \lambda, \sigma \mid g)$ and its MCMC simulation for a stable and reliable solution. For the purpose of the simulation, $\lambda^{(0)} = 1$, $\sigma^{(0)} = 0.1$, and zero vectors for $U^{(0)}$ are used for the initial values of the algorithm. A small value 10^{-1} is chosen for the pairs of parameters (α_1, β_1) and (α_2, β_2). For MCMC simulation, $50,000$ samples were generated and the last $25,000$ samples are used to estimate statistics such as mean and standard deviations for U. The MCMC results are illustrated in Figure 10.

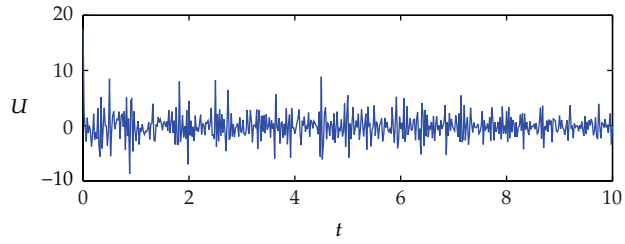

(a) Without BK

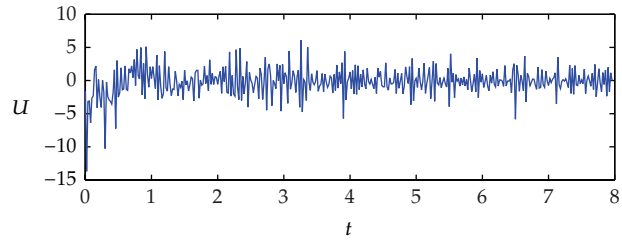

(b) With BK

Figure 9: Inverse solutions through least-squares estimation.

The upper and lower dotted lines denote the 95% credible interval, quantifying the degree of uncertainties in the solution given the measurements. The mean estimate of the posterior density is fairly stable compared with the results in Figure 9. The result in Figure 10 describes the relative likelihood for the multivariate random variable U, which includes information of the unknown nonlinear damping moments. The posterior mean represents the most probable value of the stochastic inverse model $p(U, \lambda, \sigma \mid g)$. The confidence interval can be interpreted as an indicator of the reliability of the estimated value conditional on the measured data.

It is worth to note that MCMC simulation takes a while to properly sample the target distribution. In this study, we used the evolution of components to check if the chain works properly. Figure 11 shows an example of trace plots for the marginal distribution of the MCMC result for the trial with BK. Trace plots of each component are clearly in the burn-in phase, that is, stationary states. This implies that the posterior density $p(U, \lambda, \sigma \mid g)$ is successfully explored with the designed MCMC algorithm.

Once the probability density function $p(U, \lambda, \sigma \mid g)$ is estimated, the nonlinear damping moment can then be identified by $E[p(U(t;\xi) \mid g)] = -\widetilde{B}(\dot{\phi}(t))$. The identified nonlinear roll damping moments are shown in Figure 12. It is worthwhile to note that the present method is fully nonparametric. Thus, the information of nonlinear damping moment is first revealed by a set of data based on the most probable value of the estimated function U. The set of scattered points is then used to specify the nonlinear model for damping moment. Here, the form $\widetilde{B}(\dot{\phi}(t)) = B_1\dot{\phi} + B_3\dot{\phi}^3$ is used to fit the identified data. The units of the coefficients are $[s^{-1}]$ for B_1 and $[s]$ for B_3.

It is also important to check the accuracy of the identified model. For this purpose, the roll motion is resimulated by using the identified damping moment. Figure 13 shows the comparison between the re-simulated and the measured roll responses for both cases. It is confirmed that the both trials are in well coincidence with the measured roll response.

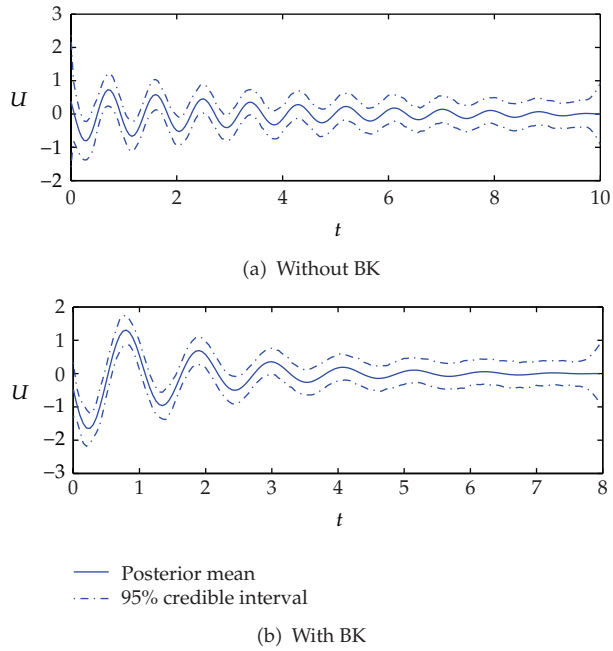

Figure 10: Solutions from stochastic inverse modeling with MCMC simulation.

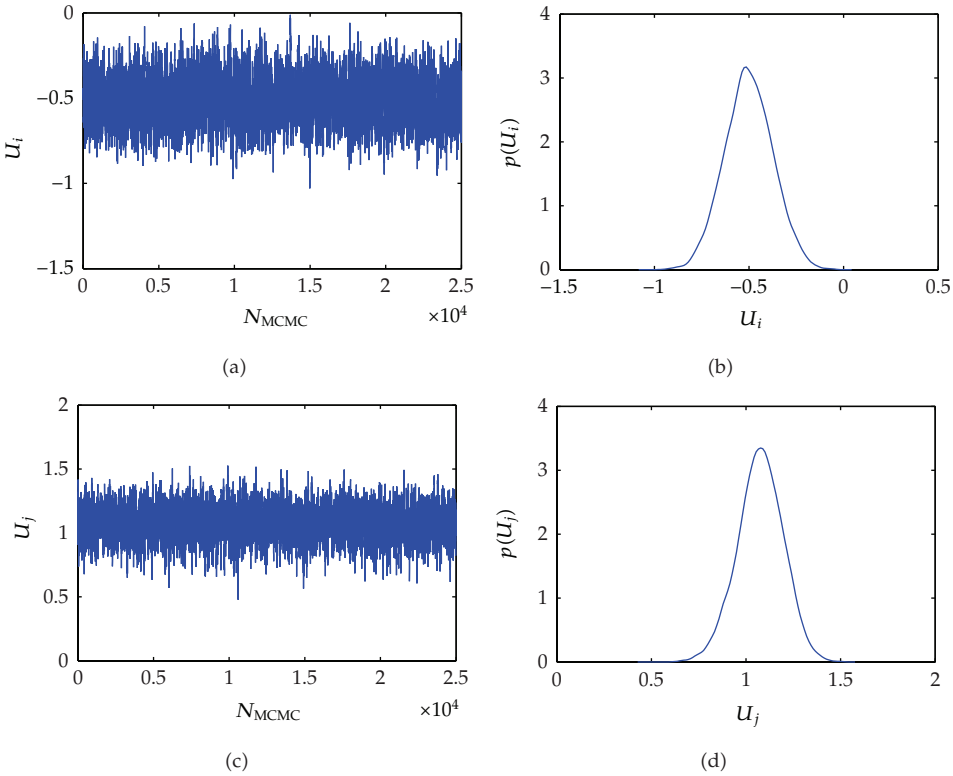

Figure 11: Typical examples of the trace plots for two components.

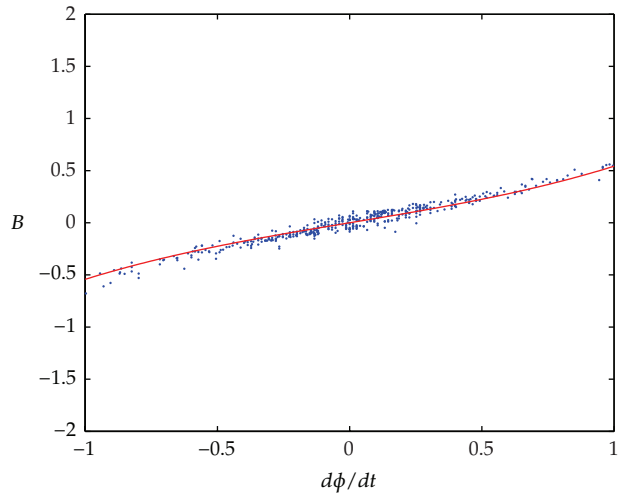

(a) Without BK

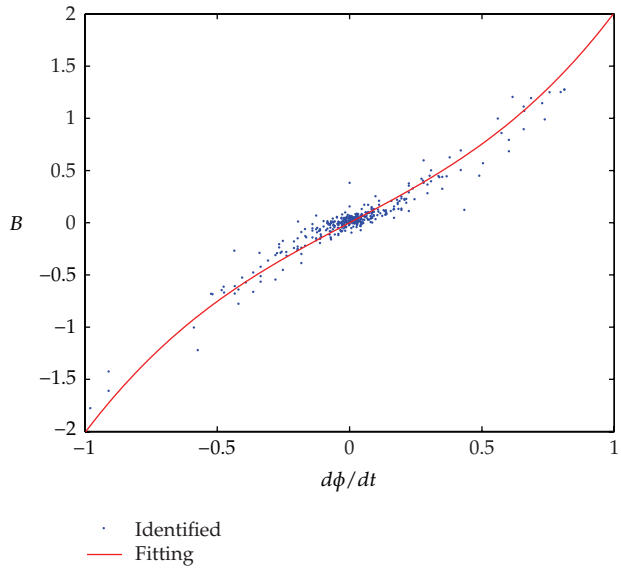

(b) With BK

Figure 12: Identified nonlinear roll damping moments.

Finally, the preceding procedures are applied to all other experimental data for the case of free-decay rolling motion. The results are summarized in Table 2. The results clearly illustrate the effect of increasing forward speed on the roll damping moments. Furthermore, the damping moment obtained with the trials with BK is much larger than those of trials without BK.

It can be naturally concluded, based on the identified results in Table 2, that it would be possible to develop an empirical formula for the nonlinear damping moments as the form:

$$\widetilde{B}(\dot{\phi}(t)) = B_1\dot{\phi} + B_3\dot{\phi}^3 = B_0\left(1 + \kappa(\mathrm{Fr})^2\right)\dot{\phi} + B_3\dot{\phi}^3, \tag{4.3}$$

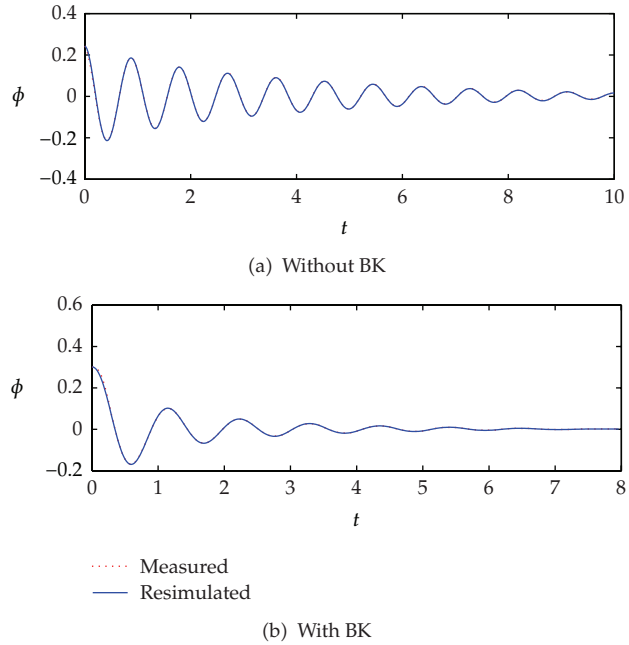

Figure 13: Resimulated roll response with the identified damping moment.

Table 2: Identified nonlinear damping for the case of free-decay rolling.

Fr	Trials with BK		Trials without BK	
	B_1	B_3	B_1	B_3
0	0.3796	0.1436	1.2408	0.6682
0.1	0.5070	0.1016	1.2475	0.4852
0.2	0.4203	0.1219	1.3262	0.6725
0.3	0.7208	0.2027	2.5105	0.4689
0.4	1.1007	0.1829	3.1812	0.6552

where B_0 is the linear contribution for zero-forward speed. The value of κ, which can be determined by fitting the identified results in Table 2, was turned out to be $\kappa = 4.7536$ for the non-BK model and $\kappa = 13.097$ for BK model, see Figure 14. It can be found that the effect of forward speed is much greater in the case of the BK model.

4.2. Periodic Motion: Forced Rolling Motion

As a second application, a periodic forced motion induced by periodic excitation is considered. The monofrequency periodic motion is imposed while ship is moving with a forward speed V:

$$\phi(t) = A_1 \cos(\omega t). \tag{4.4}$$

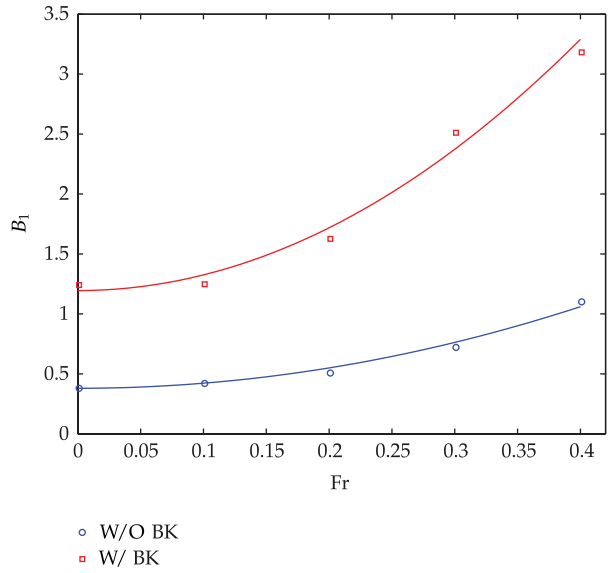

Figure 14: Determination of the coefficient κ for empirical formula.

The corresponding roll exciting moment $M(t)$ is then measured with the load cell as explained in Section 3. It is worth to point out that, in applying the proposed method to forced rolling motion, it is first necessary to know roll moment of inertia unlike free-roll decay test. The values were determined a priori through the related tests.

For the forced oscillation test, the frequency-dependent coefficients of the roll moment of inertia are generally obtained by Fourier analysis:

$$(I + \Delta I) = \frac{KA_1 - M_a \cos(\varepsilon)}{\omega^2 A_1}, \tag{4.5}$$

where M_a is the amplitude of the exciting moment, ε is the phase difference between the roll angle and the exciting moment, and ω is the exciting frequency. The obtained coefficients are illustrated in Figure 15.

Now we are ready to apply the present method to the measured data. For illustrating purposes, a particular case of experimental data was chosen as identification examples for the forced rolling motion. Figure 16 shows the measured roll response and the exciting moment for the test model with BK when Fr = 1.0 and exciting frequency $\omega = 5.12$. Figure 17 shows the step-by-step results of identifying roll damping moment from the measured data. The measured data was first converted to the observable parameter g through (2.7). The converted quantity, illustrated in Figure 17(a), leads to the construction of stochastic inverse model as in (2.13). Without loss of generality, the same conditions were used to explore the constructed stochastic inverse model for the MCMC algorithm as explained in Section 4.1. The MCMC results were shown in Figure 17(b). Next, the roll response is resimulated with the identified inverse solution. The result is shown in Figure 17(c). It is observed that the re-simulated response is in good agreement with the measured roll response. This proves the accuracy of the identified roll damping moment.

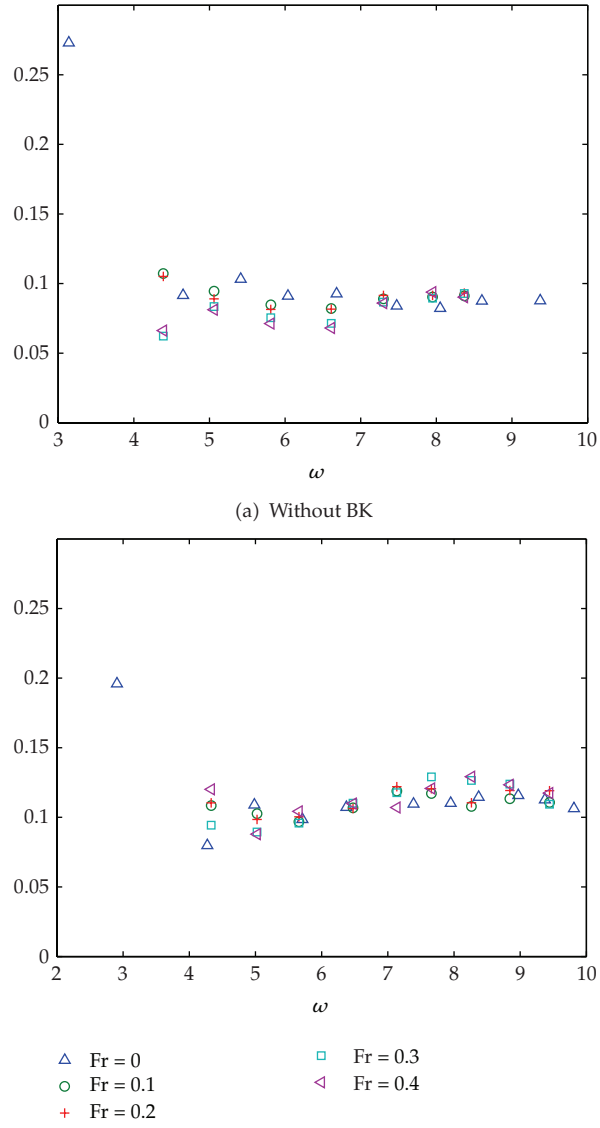

Figure 15: Nondimensional moment of inertia of the test model: $(I + \Delta I)/mB^2$.

It is worth noting here that, for the case of free-decay rolling motion, the effects on roll amplitude in a roll-decay are mainly due to the damping [28], but the same cannot be said in the case of forced rolling motion. It could be expected that the nonlinearity in the restoring plays a role and the estimated damping moment is not dependent only on the roll angular velocity. Consequently, it is difficult to build an analytical model of the identified nonlinear damping moment unlike the case of free-decay rolling motion as described in Section 4.1.

Instead, we performed here a quantitative analysis of the results obtained by applying the preceding procedure to all other experimental data of the forced rolling motion. The rationale behind this is that the relating results can be considered to be periodic with the

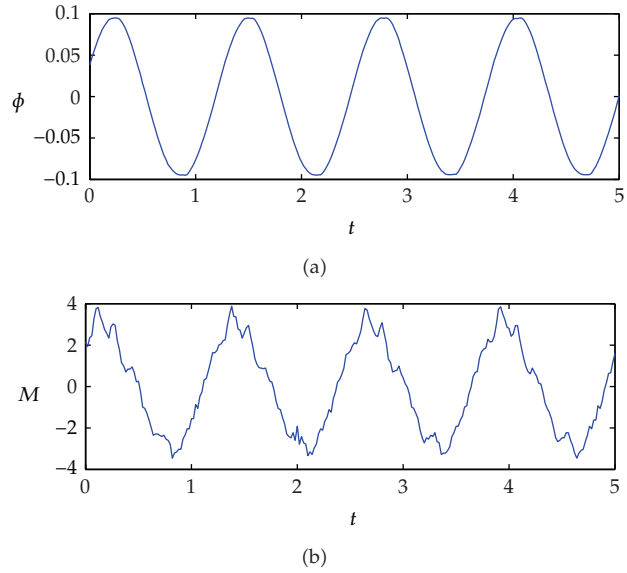

Figure 16: Measured roll response and exciting moment.

exciting frequency since the monofrequency periodic motion was imposed. It is convenient to illustrate and compare the results in terms of frequency for this case. Figures 18 and 19 show the peak values of the identified solution from the present stochastic identification procedure. For all cases, the same amplitude of the motion is imposed. It should be noted that the function U includes the information on the damping moment. That is, the results in Figures 18 and 19 can be explained by the fact that the damping moment is dependent on the forward speed and the exciting frequency.

5. Conclusions

In this paper, a stochastic inverse method has been investigated for the identification of roll characteristics of a ship moving at nonzero-forward speeds. The rolling motion has been treated as a single-degree-of-freedom nonlinear equation of motion, uncoupled from other motions. On this basis, the stochastic inverse model for the nonlinear damping moment was derived as a probabilistic expression in terms of the observable parameter which is a function of the measurements of the roll angle and excitation. The stochastic inverse model contains the information of the nonlinear damping contribution as the multivariate random variables. Given measured data, the nonlinear damping moments were identified through the designed Markov chain Monte Carlo algorithm.

To ensure applicability, the proposed method has been applied to the experimental data for the two different mechanical phenomena regarding ship roll motions, that is, the transient motion and forced periodic motion. In nonlinear system identification, it is difficult to define the quality of the identified results because it depends on its purposes. The aim of the present study is to find the nonlinear system model which can reproduce the measured system response. In this sense, it can be concluded that the proposed method

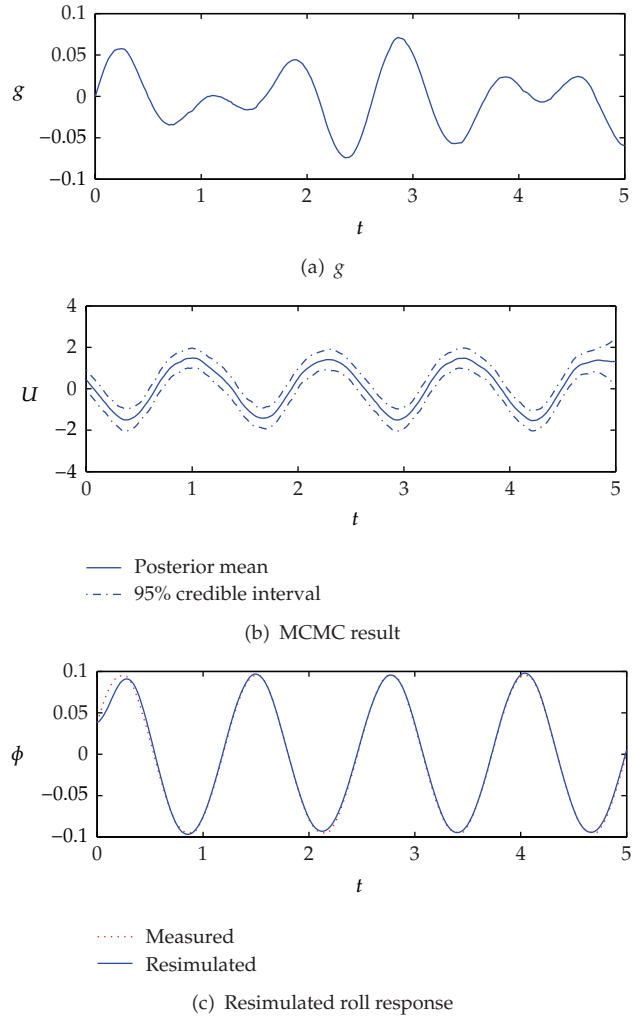

Figure 17: Step-by-step result for the identification of roll damping moment.

can accurately identify the nonlinearity in damping of a ship moving at nonzero-forward speeds.

The preset stochastic inverse method has the following limitations. Firstly, the method is derived based on the assumption of small amplitude of the rolling motion so that the restoring moment can be approximated by the linear form. In reality, the restoring moment is also nonlinear. The nonlinear contribution cannot be neglected. The extension to a system with the nonlinear restoring is not difficult mathematically. However, the new formulation needs additional information on the restoring nonlinearity for the identification purpose. Secondly, the experimental setups do not strictly reflect the actual motion of the ship. Rolling motion is generally coupled with other motions, such as sway and heave. In reality, the coupling effects should also be taken into account. However, for simplicity of the experimental application, in this paper, the test model was restrained in all degrees of motion except the roll motion while the model was moving at a constant speed.

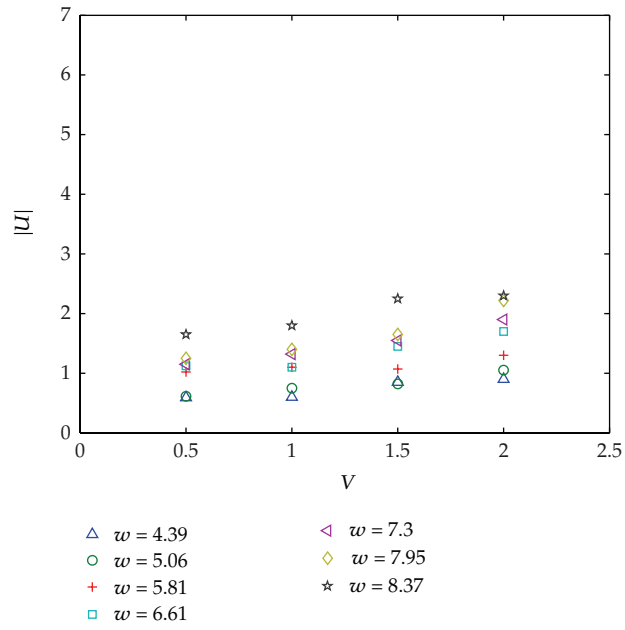

(a) Identified solution versus forward speed

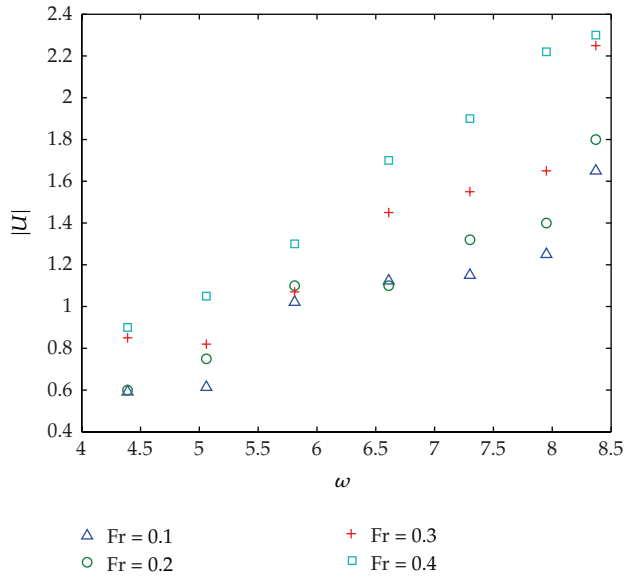

(b) Identified solution versus exciting frequency

Figure 18: Illustration of the peak value of the identified result for the trial without BK.

Acknowledgments

The authors would like to thank the editor and anonymous reviewers for their valuable comments, suggestions, and constructive criticism, which were very helpful in improving the paper substantially.

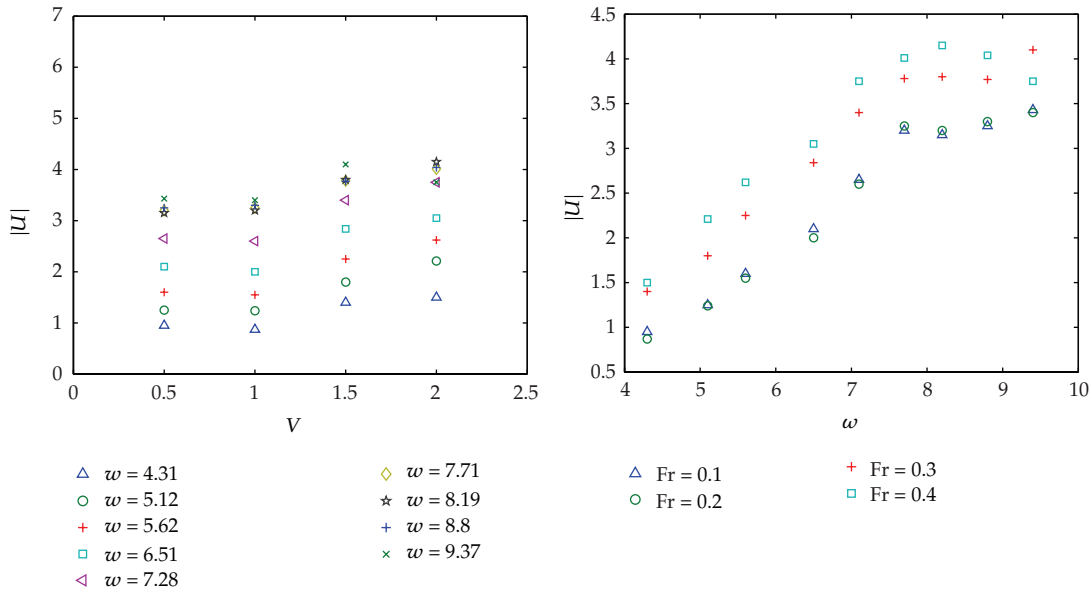

(a) Identified solution versus forward speed

(b) Identified solution versus exciting frequency

Figure 19: Illustration of the peak value of the identified result for the trial with BK.

References

[1] S. L. Han and T. Kinoshita, "Nonlinear damping identification in nonlinear dynamic system based on stochastic inverse approach," *Mathematical Problems in Engineering*, vol. 2012, Article ID 574291, 2012.

[2] S. L. Han and T. Kinoshita, "Stochastic inverse modeling of nonlinear roll damping moment of a ship," *Applied Ocean Research*, vol. 39, pp. 11–19, 2013.

[3] R. Bhattacharyya, *Dynamics of Marine Vehicles*, John Wiley and Sons, New York, NY, USA, 1978.

[4] S. N. Blagoveshchensky, *Theory of Ship Motions, vols. I and II*, Dover Publications, New York, NY, USA, 1962.

[5] J. O. De Kat and J. R. Paulling, "The simulation of ship motions and capsizing in severe seas," *Transactions of SNAME*, vol. 117, pp. 127–135, 1989.

[6] A. Zborowski and M. Taylan, "Evaluation of small vessels' roll motion stability reserve for resonance conditions," in *Proceedings of the 14th Ship Technology and Research STAR Symposium 1989 in conjunction with the SNAME Spring Meeting*, New Orleans, La, USA, April 1989.

[7] J. A. Witz, C. B. Ablett, and J. H. Harrison, "Roll response of semisubmersibles with non-linear restoring moment characteristics," *Applied Ocean Research*, vol. 11, no. 3, pp. 153–166, 1989.

[8] J. F. Dalzell, "A note on the form of ship roll damping," *Journal of Ship Research*, vol. 22, no. 3, pp. 178–185, 1978.

[9] J. B. Roberts, "Estimation of nonlinear ship roll damping from free-decay data," *Journal of Ship Research*, vol. 29, no. 2, pp. 127–138, 1985.

[10] J. B. Mathisen and W. G. Price, "Estimation of ship roll damping coefficients," *RINA Transaction*, vol. 127, pp. 169–186, 1985.

[11] D. W. Bass and M. R. Haddara, "Nonlinear models of ship roll damping," *International Shipbuilding Progress*, vol. 35, no. 401, pp. 5–24, 1988.

[12] J. R. Spouge, "Non-linear analysis of large-amplitude rolling experiments," *International Shipbuilding Progress*, vol. 35, no. 403, pp. 271–320, 1988.

[13] H. S. Y. Chan, Z. Xu, and W. L. Huang, "Estimation of nonlinear damping coefficients from large-amplitude ship rolling motions," *Applied Ocean Research*, vol. 17, no. 4, pp. 217–224, 1995.

[14] Y. Himeno, "Prediction of ship roll damping—a state of the art," Tech. Rep. 239, Department of Naval Architecture and Marine Engineering, University of Michigan, Ann Abor, Mich, USA, 1981.

[15] M. Taylan, "The effect of nonlinear damping and restoring in ship rolling," *Ocean Engineering*, vol. 27, no. 9, pp. 921–932, 2000.

[16] M. R. Haddara and M. Hinchey, "On the use of neural network techniques in the analysis of free roll decay curves," *International Shipbuilding Progress*, vol. 42, pp. 166–178, 1995.

[17] M. R. Haddara and M. Wishahy, "An investigation of roll characteristics of two full scale ships at sea," *Ocean Engineering*, vol. 29, no. 6, pp. 651–666, 2002.

[18] J. B. Roberts and M. Vasta, "Markov modelling and stochastic identification for nonlinear ship rolling in random waves," *Philosophical Transactions of the Royal Society A*, vol. 358, no. 1771, pp. 1917–1941, 2000.

[19] T. S. Jang, H. S. Choi, and S. L. Han, "A new method for detecting non-linear damping and restoring forces in non-linear oscillation systems from transient data," *International Journal of Non-Linear Mechanics*, vol. 44, no. 7, pp. 801–808, 2009.

[20] T. S. Jang, J. W. Son, S. L. Han, H. G. Sung, S. K. Lee, and S. C. Shin, "A numerical investigation on nonparametric identification of nonlinear roll damping moment of a ship from transient response," *The Open Ocean Engineering Journal*, vol. 3, pp. 100–107, 2010.

[21] A. Kirsch, *An Introduction to the Mathematical Theory of Inverse Problems*, vol. 120, Springer, New York, NY, USA, 1996.

[22] C. W. Groetsch, *Inverse Problems in the Mathematical Sciences*, Informatica International, 1993.

[23] J. Kaipio and E. Somersalo, *Statistical and Computational Inverse Problems*, Springer, New York, NY, USA, 2005.

[24] J. Wang and N. Zabaras, "Hierarchical Bayesian models for inverse problems in heat conduction," *Inverse Problems*, vol. 21, no. 1, pp. 183–206, 2005.

[25] J. Wang and N. Zabaras, "A Markov random field model of contamination source identification in porous media flow," *International Journal of Heat and Mass Transfer*, vol. 49, no. 5-6, pp. 939–950, 2006.

[26] C. Andrieu, N. De Freitas, A. Doucet, and M. I. Jordan, "An introduction to MCMC for machine learning," *Machine Learning*, vol. 50, no. 1-2, pp. 5–43, 2003.

[27] M. R. Haddara and S. Zhang, "Effect of forward speed on the roll damping of three small fishing vessels," *Journal of Offshore Mechanics and Arctic Engineering*, vol. 116, no. 2, pp. 102–108, 1994.

[28] G. Bulian, "Estimation of nonlinear roll decay parameters using an analytical approximate solution of the decay time history," *International Shipbuilding Progress*, vol. 51, pp. 5–32, 2004.